Nébuleuses de (vents de) pulsars
(PWNe, ou “plérions”)

Yves Gallant

LUPM, CNRS / IN2P3, U. Montpellier 2

École “Astronomie gamma”
Observatoire de Haute-Provence, le 26 mai 2011

Galactic TeV γ-ray sources and PWNe

- much improved sensitivity of current generation of Imaging Atmospheric Cherenkov Telescopes (IACTs), inaugurated by HESS (initial 4-telescope array completed >7 years ago)
- HESS Galactic plane survey : longitudes $\ell \approx -80°$ to $60°$

(Chaves, H.E.S.S., 2009 ICRC)

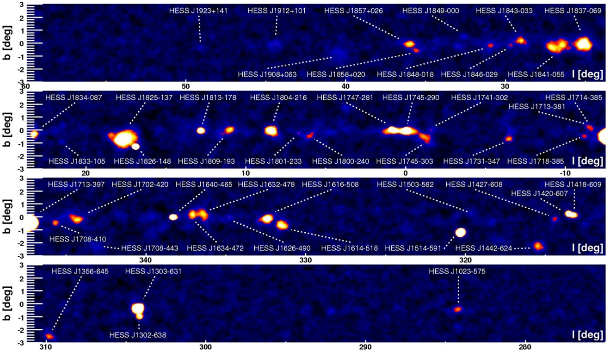

- currently about 70 Galactic TeV sources known
- roughly half are identified as PWNe or candidate PWNe
- PWNe may be dominant sources of high-energy $e^{\pm}$ cosmic rays

Plan du cours

Introduction : the Crab Nebula

- by far the most intensively studied pulsar wind nebula, both by observations at all wavebands and theoretically
- remnant of SN 1054
- filaments (emission lines) : expanding SN ejecta
- bluish continuum : **sychrotron** emission from relativistic e^- (Shklovskii 195x)
- strong polarisation : ordered magnetic field

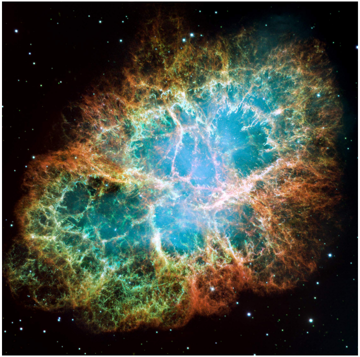

ESO/VLT (true colour)

- magnetic field and particles thought to originate in a spinning central object (Piddington 1957), hypothesized to be a neutron star (Pacini 1967)
- Crab pulsar discovery (Middleditch et al. 1969) confirmed scenario

The Crab Nebula in synchrotron emission

- one of brightest sources in the sky in major parts of the electromagnetic spectrum :

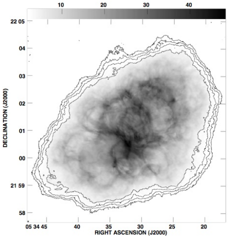

radio (VLA)

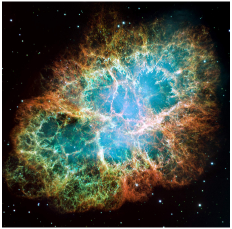

optical (ESO/VLT)

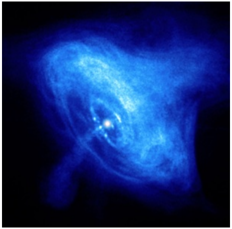

X-rays (*Chandra*)

- polarisation also in radio, X-rays...
- synchrotron more concentrated around pulsar in X-rays than in optical, and in optical than radio

Synchrotron spectrum of the Crab Nebula

- total energy flux $F_\nu \equiv \mathrm{d}F/\mathrm{d}\nu$, in $\mathrm{erg\,cm^{-2}\,s^{-1}\,Hz^{-1}}$
- plot spectral energy distribution as $\nu F_\nu = \mathrm{d}F/\mathrm{d}(\ln\nu)$

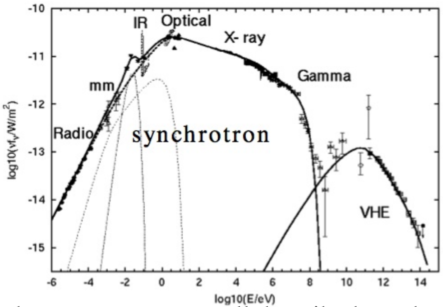

(Horns et al. 2004)

- synchrotron spectrum well described as a broken **power law** :

$$F_\nu = \begin{cases} F_0\,\nu^{-s_0} & , \quad \nu < \nu_{01} \\ F_1\,\nu^{-s_1} & , \quad \nu_{01} < \nu < \nu_{12} \\ F_2\,\nu^{-s_2} & , \quad \nu_{12} < \nu \end{cases}$$

- spectral break frequencies ν_{01} in IR, ν_{12} in UV (peak in νF_ν)
- full description requires additional break ν_{23} in soft γ-rays, and cutoff below GeV energies

Particles and magnetic field

- sychrotron emission : relativistic e^- (or e^+) of Lorentz factor γ radiate power

$$P_{\text{sync}} = \frac{1}{6\pi}\sigma_{\text{T}} c B^2 \gamma^2 \equiv P_B \gamma^2 \,,$$

with spectrum peaking at

$$\nu_{\text{sync}} = \frac{f}{2\pi}\,\frac{eB}{m_e c}\,\gamma^2 \equiv f \nu_B \gamma^2 \,, \quad \text{where} \quad f \approx 0.29 \times \frac{3}{2} = 0.44$$

- *if B uniform*, can infer source particle spectrum $N(\gamma) \equiv \mathrm{d}N/\mathrm{d}\gamma$

$$N(\gamma) = \begin{cases} N_0\, \gamma^{-p_0} & , \quad \gamma < \gamma_{01} \\ N_1\, \gamma^{-p_1} & , \quad \gamma_{01} < \gamma < \gamma_{12} \\ N_2\, \gamma^{-p_2} & , \quad \gamma_{12} < \gamma \end{cases}$$

with $p_i = 2s_i + 1$, and in δ-function approximation $P_{\text{sync}}\delta(\nu - \nu_{\text{sync}})$

$$N_i = \frac{8\pi f \nu_B}{P_B}\,(f\nu_B)^{-s_i}\, D^2 F_i \;\propto\; B^{-s_i - 1}\, D^2\, F_i$$

Total energy and number of $e^{\pm}$

N.B. "electrons" refers to both e^- and e^+, unless otherwise noted

- energy predominantly carried by electrons with γ near γ_{01}

$$E_{\rm elec} = \int_{\gamma_{\rm min}}^{\gamma_{\rm max}} m_e \gamma c^2 \, N(\gamma) {\rm d}\gamma \; \approx m_e c^2 N_0 \gamma_{01}^{2-p_0} \left(\frac{1}{2-p_0} + \frac{1}{p_1-2} \right)$$

- electron energy distribution $m_e c^2 \, \gamma^2 \, N(\gamma) = {\rm d}E_{\rm elec}/{\rm d}(\ln \gamma)$:

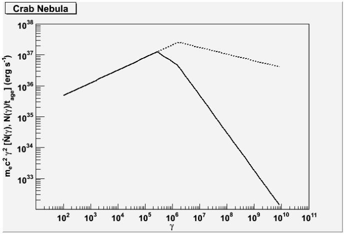

Energy distribution

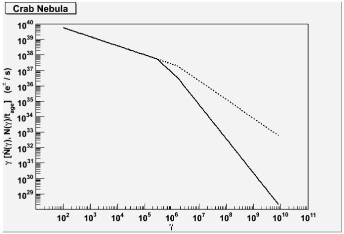

Number distribution

- electron number distribution $\gamma N(\gamma) = {\rm d}N/{\rm d}(\ln \gamma)$
- total number dominated by electrons with γ near $\gamma_{\rm min}$

$$N_{\rm elec} = \int_{\gamma_{\rm min}}^{\gamma_{\rm max}} N(\gamma) {\rm d}\gamma \; \approx \; N_0 \, \gamma_{\rm min}^{1-p_0} \, \frac{1}{p_0-1}$$

Equipartition estimate for magnetic field

- for nebula of angular radius θ at distance D, magnetic energy

$$E_B = \frac{4\pi}{3}\theta^3 D^3 \cdot \frac{B^2}{8\pi} = \frac{1}{6}\theta^3 D^3 B^2$$

- magnetic field estimate assuming *equipartition* $E_B = E_{\rm elec}$

$$B_{\rm eq} \approx \left[54\sqrt{2\pi f}\,\frac{m_e^{5/2}c^{9/2}}{e^{7/2}}\left(\frac{1}{2-p_0}+\frac{1}{p_1-2}\right)F_0\,\nu_{01}^{1/2-s_0}\,\frac{1}{D\,\theta^3}\right]^{2/7}$$

$$= 280\,\mu\mathrm{G} \qquad \text{for the Crab Nebula}$$

- roughly motivated by fact that relativistic gas and magnetic pressures must become comparable away from inner nebula
- minimum-energy magnetic field estimate gives similar value

- with this magnetic field, $E_{\rm elec} = E_B = 1.2 \times 10^{48}$ erg
- using $\nu_{\rm min} \approx 10^7$ Hz, yields $N_{\rm elec} \approx 3 \times 10^{50}$

- for constant injection, requires $\dot N_{\rm elec} > 10^{40} e^{\pm}$/s, and $\dot E_{{\rm elec}+B} > 0.8 \times 10^{38}$ erg/s (vs pulsar $\dot E = 4.6 \times 10^{38}$ erg/s)

Synchrotron losses and spectral break

- electron loses energy at rate $m_e\dot{\gamma}c^2 = -P_B\gamma^2 \Rightarrow$ *cooling time*

$$t_{\rm cool}(\gamma) \equiv \frac{\gamma}{\dot{\gamma}} = 6\pi\frac{m_e c}{\sigma_{\rm T}}\frac{1}{B^2\,\gamma} = 3\frac{\sqrt{2\pi f m_e c\, e}}{\sigma_{\rm T}}B^{-3/2}\,\nu_{\rm sync}^{-1/2}\ ,$$

- for synchrotron X-rays, $h\nu = 1\,{\rm keV}$, $t_{\rm cool} = 12\,{\rm yr}$ if $B = 280\,\mu{\rm G}$

- for steady injection of a power-law spectrum, $\dot{N}(\gamma) = \dot{N}_0\gamma^{-p}$: **broken power law**, with $\gamma_{\rm cool}$ such that $t_{\rm cool}(\gamma_{\rm cool}) \equiv t_{\rm age}$

$$N(\gamma) \approx \begin{cases} \dot{N}_0 t_{\rm age}\,\gamma^{-p} & ,\quad \gamma \ll \gamma_{\rm cool}\ , \\ \dot{N}_0 t_{\rm age}\gamma_{\rm cool}\gamma^{-(p+1)} & ,\quad \gamma \gg \gamma_{\rm cool}\ . \end{cases}$$

- break energy $\gamma_{\rm cool}$ corresponds to *cooling break* frequency

$$\nu_{\rm cool} = 18\pi f\,\frac{e\,m_e c}{\sigma_{\rm T}^2}\,\frac{1}{B^3\,t_{\rm age}^2} = 7.4\times10^{17}\,B_{\rm nT}^{-3}\ t_{\rm kyr}^{-2}\ {\rm Hz}\ ,$$

- for the Crab, $B_{\rm eq} = 280\,\mu{\rm G}$ yields $\nu_{\rm cool} \approx 3\times10^{13}\,{\rm Hz} \approx \nu_{01}$
- higher-frequency ν_{12} must then be intrinsic, *injection break*

Inverse Compton emission

- Crab Nebula γ-ray spectrum above several 100 MeV generally interpreted as **inverse Compton** (IC) emission (although hadronic contribution also proposed, e.g. Horns et al. 2007)

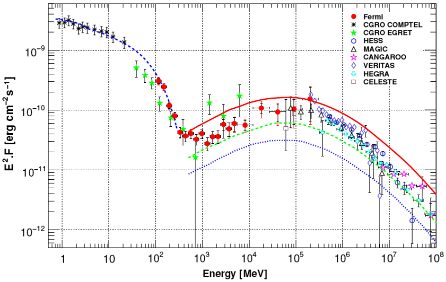

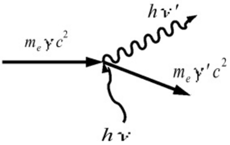

$$h\nu' \approx \frac{4}{3}\gamma^2 h\nu_{\rm ph}$$

- in Thomson regime, power scattered by each electron is

$$P_{\rm IC} = \frac{4}{3}\sigma_{\rm T} c U_{\rm ph}\gamma^2 = \left(\frac{U_{\rm ph}}{U_B}\right) P_{\rm synch}, \quad \text{where} \quad U_B = \frac{B^2}{8\pi}$$

Caveat: Klein-Nishina effects reduce cross-section at high energies

- allows determination of $\langle B \rangle$ from $U_{\rm ph}$ (when comparing same γ)
- using Atoyan & Aharonian (1996), $100\,\mu$G $< \langle B \rangle <$ $200\,\mu$G

Target photons for IC emission

Target photon U_{ph} components:

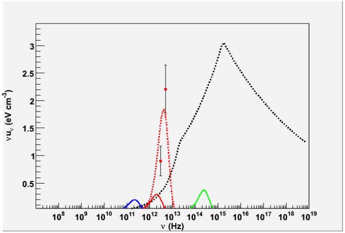

1. Cosmic Microwave Background
2. Galactic IR background, $T \sim 25\,\mathrm{K}$
3. stellar background, $T \sim 4000\,\mathrm{K}$
4. Nebular dust emission, $T \sim 40\,\mathrm{K}$
5. Nebular synchrotron photons

- first three components essentially uniform on scale of nebula
- Galactic backgrounds modelled e.g. by Porter et al. (2006)

- in Crab Nebula, local components 4 and especially 5 dominate (*synchrotron self-Compton* or SSC emission)
- the Crab also seems to be unusal among pulsar wind nebulae in that $\langle B \rangle$ close to B_{eq} (in other PWNe, often find $\langle B \rangle \ll B_{\mathrm{eq}}$)

Young PWNe and composite SNRs

- pulsars are born in (core-collapse) supernovae (type II / Ib,c)
- Crab Nebula unusual in that SN remnant shock not detected : purely "**plerionic**" (center-filled) SNR
- more generally, PWNe inside classical, **shell-type** SNR : "**composite**" SNR

X-ray (*Chandra*) images

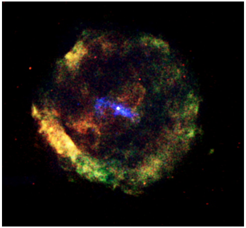

G 11.2–0.3

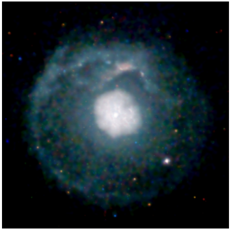

G 21.5–0.9

Kes 75

- thermal X-ray emission from shocked supernova ejecta
- non-thermal (synchrotron) emission near two acceleration sites :
  - blast wave of initial explosion : SNR shell (forward shock)
  - pulsar (wind termination shock) : pulsar wind nebula

Structure of a young composite SNR (I)

- "free expansion" phase : PWN and SNR evolution decoupled

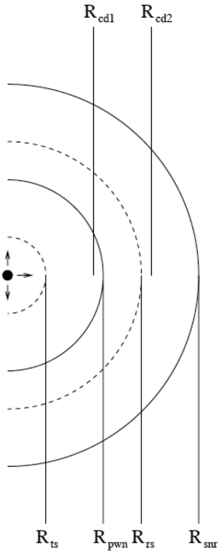

- 4 shocks : $R_{\mathrm{ts}}, R_{\mathrm{pwn}}, R_{\mathrm{rs}}, R_{\mathrm{snr}}$
- relativistic pulsar wind ends at R_{ts}
- post-shock pulsar wind : synchrotron and inverse Compton emission (PWN)
- shocked ejecta, Rayleigh-Taylor unstable contact discontinuity R_{cd1} : Crab filaments
- expansion drives shock R_{pwn} into cold ejecta
- reverse shock R_{rs} heats ejecta from larger radii
- contact discontinuity R_{cd2} with shocked interstellar or circumstellar medium
- blast wave R_{snr} into surrounding medium

- van der Swaluw et al. (2001) : 1D, spherical symmetry assumption

Structure of a young composite SNR (II)

- relativistic hydrodynamics simulations (e.g. Bucciantini et al. 2003)

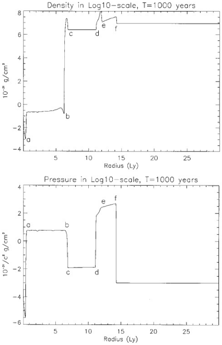

- 4 shocks : $R_{\rm ts}(a), R_{\rm pwn}(c), R_{\rm rs}(d), R_{\rm snr}(f)$
- relativistic pulsar wind ends at $R_{\rm ts}$
- post-shock pulsar wind : synchrotron and inverse Compton emission (PWN)
- shocked ejecta, Rayleigh-Taylor unstable contact discontinuity $R_{\rm cd1}(b)$: Crab filaments
- expansion drives shock $R_{\rm pwn}$ into cold ejecta
- reverse shock $R_{\rm rs}$ heats ejecta from larger radii
- contact discontinuity $R_{\rm cd2}(e)$ with shocked interstellar or circumstellar medium
- blast wave $R_{\rm snr}$ into surrounding medium

- MHD simulations show same evolution outside $R_{\rm cd1}$ for same $\dot{E}$

TeV (and GeV) γ-ray emitting young PWNe

- in addition to the **Crab**, HESS discovered TeV emission from composites **G 0.9+0.1** (A&A, **432**, L25, 2005), **G 21.5–0.9** and **Kes 75** (Djannati-Ataï et al. 2007, ICRC, `arXiv:0710.2247`)
- *VERITAS* discovery of TeV emission from plerion **G 54.1+0.3** (Acciari et al. 2010, *ApJ* **719**, L69)

- **MSH 15–52** : first PWN angularly resolved in TeV γ-rays (*HESS*, A&A **435**, L17, 2005)
- *Fermi*-LAT detection (ApJ **714**, 927, 2010)
- contours: ROSAT
- X-ray thermal shell and non-thermal "jet-like" nebula
- TeV morphology matches X-ray PWN

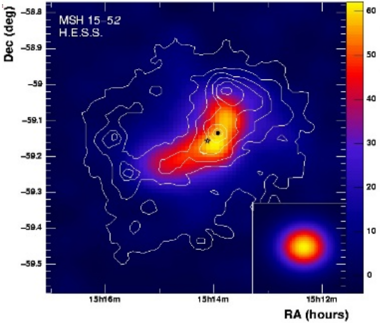

- IC emission $\propto$ (approximately uniform) target photon density $\Rightarrow$ direct inference of spatial distribution of electrons

Young composite SNR discovered in γ-rays

The progressive identification of **HESS J1813–178**

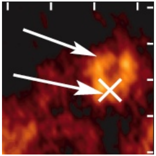

- *XMM* revealed an extended non-thermal nebula inside the shell (Funk et al. 2007a)

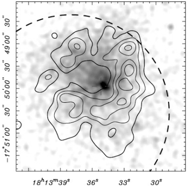

- *XMM* found pulsed emission, $\dot{E} = (6.8 \pm 2.7) \times 10^{37}$ erg/s (Gotthelf & Halpern 2009)

- Brogan et al. (2005) revealed its coincidence with a shell-type radio SNR (and *ASCA* source)

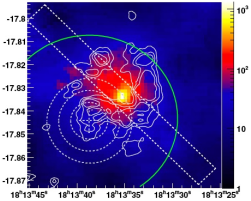

- *Chandra* revealed a pulsar candidate (Helfand et al. 2007)

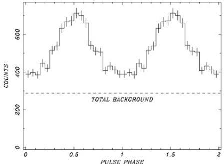

Apparent efficiency of TeV γ-ray emission

- fraction of *current* pulsar spindown luminosity $\dot{E}$ radiated into observed TeV γ-rays L_γ :

$$\varepsilon_\gamma \equiv \frac{4\pi D^2 F_{0.3-30\,\mathrm{TeV}}}{\dot{E}}$$

TeV source	PSR name	$\dot{E}$ (erg/s)	ε_γ
Crab Nebula	B0531+21	4.6×10^{38}	0.02%
HESS J1813–178	**J1813–1749**	$\sim 7 \times 10^{37}$	0.06%
G 0.9+0.1	**J1747–2809**	4.3×10^{37}	0.1%
G 21.5–0.9	J1833–1034	3.4×10^{37}	0.02%
MSH 15–52	B1509–58	1.8×10^{37}	0.4%
G 54.1+0.3	J1930+1852	1.2×10^{37}	0.2%
Kes 75	J1846–0258	0.8×10^{37}	0.3%

- ε_γ typically $\sim$0.1% for these young (age < 5 kyr) PWNe
- can be used as one criterion for the plausibility of other proposed associations

PWNe in older composite SNRs

- reverse shock eventually contacts PWN at SNR center
- PWN is initially "crushed" by shocked ejecta pressure
- in spherically symmetric simulations (e.g. MHD by Bucciantini et al. 2003), several reverberations before slower, steady expansion

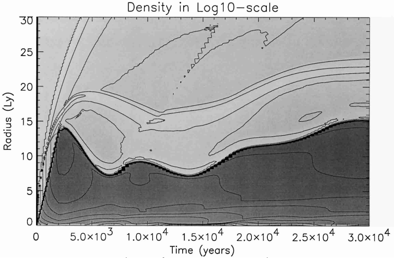

density vs r and t

2D asymmetric evolution

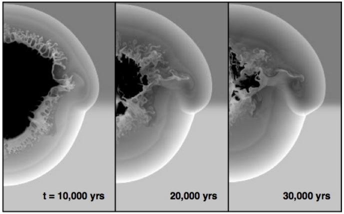

- in more realistic 2D, Rayleigh-Taylor instabilities can mix plerion and ejecta (Blondin, Chevalier & Frierson 2001)
- asymmetries in medium can shift or "offset" PWN from pulsar
- eventually settles to "subsonic" expansion inside Sedov-phase remnant (e.g. van der Swaluw et al. 2001)

γ-rays from older, "offset" PWNe

- TeV emission from **Vela X** nebula (*HESS*, A&A **448**, L43, 2006); also *Fermi*-LAT detection (ApJ **713**, 146, 2010)

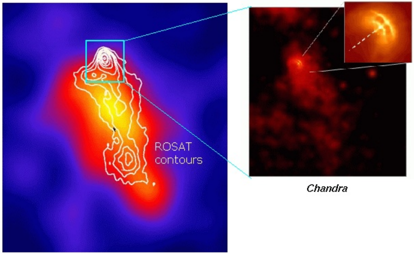

- coincident with one-sided "jet" (Markwardt & Ögelman 1995)
- compact X-ray nebula not conspicuous in TeV γ-rays $\Rightarrow$ torii and jets bright in X-rays because of higher magnetic field
- offset morphology due to passage of anisotropic reverse shock?

- two TeV PWNe in **Kookaburra** appear to fall in same category
- radio / X-ray nonthermal emission matching **HESS J1356–645** places it in same category (Renaud et al., *HESS* 2008)

PWN established from TeV properties

- previous identifications based on positional and morphological match to known X-ray or radio PWNe

HESS J1825–137 as nebula of PSR B1823–13

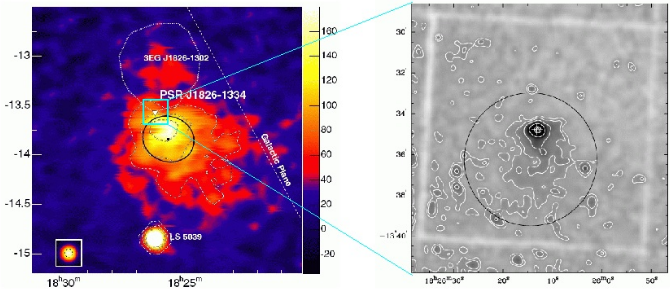

HESS (A&A **460**, 365, 2006) XMM (Gaensler et al. 2003)

- large TeV source, offset from PSR B1823–13 position
- smaller X-ray extension, E–W compact nebula and cometary “tail” in the direction of HESS source centroid

PWN established from TeV properties

- previous identifications based on positional and morphological match to known X-ray or radio PWNe

HESS J1825–137 as nebula of PSR B1823–13

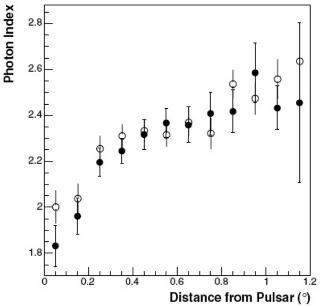

A&A **460**, 365 (2006)

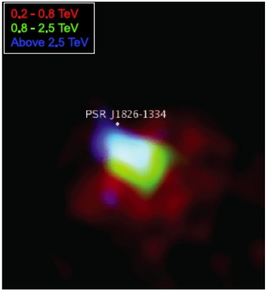

Funk et al. 2007

- TeV γ-ray spectral steepening with distance away from pulsar
- consistent with radiative losses of $e^{\pm}$ accelerated near the pulsar
- electron scattering CMB to 1 TeV radiates synchrotron $\ll$ 1 keV (for plausible B's) $\Rightarrow$ consistent smaller size of X-ray nebula

Apparent γ-ray efficiency of offset PWNe

- other PWN identified from energy-dependent morphology in TeV γ-rays : **HESS J1303–631** (Dalton et al. 2009)

TeV source	PSR name	$\dot{E}$ (erg/s)	ε_γ
Kookaburra (K3)	J1420–6048	1.0×10^{37}	0.8%
Vela X	B0833–45	6.9×10^{36}	0.01%
Rabbit	**J1418–6058**	4.9×10^{36}	$0.8\%\ d_5^2$
HESS J1356–645	J1357–6429	3.1×10^{36}	0.4%
HESS J1825–137	B1823–13	2.8×10^{36}	7%
HESS J1303–631	J1301–6305	1.7×10^{36}	7%

- offset PWNe : ε_γ typically $\sim$1%, but $\dot{E}\sim10^{36}$ erg/s

Candidate TeV γ-ray PWNe

- TeV sources classified as candidate (offset) PWNe based on:
  - positional coincidence with energetically plausible pulsar
  - but no matching (radio or X-ray) PWN, nor signficant energy-dependent TeV morphology

TeV γ-ray luminosity distribution of PWNe

- distances from ATNF pulsar catalogue, using DM and Galactic n_e model of Cordes & Lazio (2002) when no independent D

young PWNe

offset PWNe

candidate PWNe

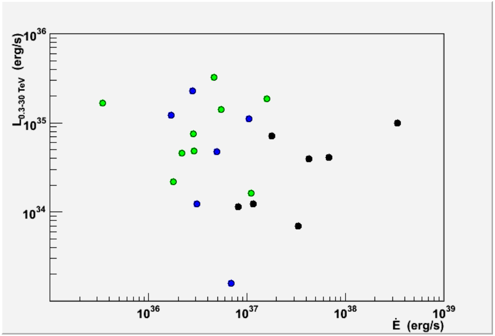

- relatively narrow range of $L_{0.3-30\,\mathrm{TeV}}$ ($\sim$2 decades); median established PWN luminosity $L_{0.3-30\,\mathrm{TeV}} \approx 4.5 \times 10^{34}$ erg/s
- no clear correlation with $\dot{E}$, nor separation between categories

TeV γ-ray and X-ray luminosities of PWNe

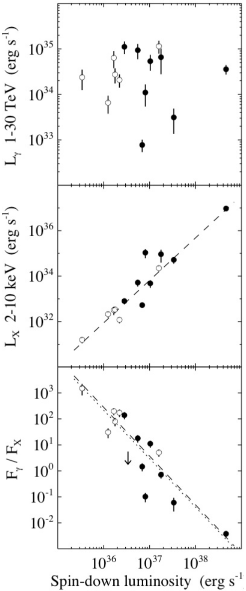

- L_{TeV} much more tightly clustered ($\sim$2 decades) than L_X (6 decades); no correlation with $\dot{E}$ (2-3 decades)
- strong correlation of L_X with $\dot{E}$, hence correlation of L_{TeV}/L_X with $\dot{E}$ (also with pulsar age τ; ratio independent of estimate for D, unlike ε) (Grenier 2009, Mattana et al. 2009)
- X-rays trace recently injected particles, whereas TeV γ-rays reflect history of injection since pulsar birth

TeV γ-ray size distribution of PWNe

- physical radius $\ell = \theta D$ based on measured (or upper limit on) intrinsic Gaussian source extension θ in TeV γ-rays

young PWNe

offset PWNe

candidate PWNe

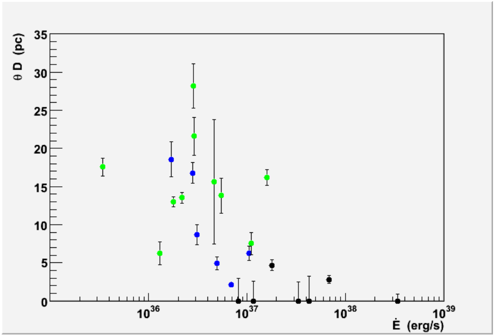

- clear trend towards larger PWN sizes at lower $\dot{E}$ (corresponding to older PWNe, larger characteristic ages)
- median established PWN $\ell \approx 3$ pc; candidate PWNe tend to be larger $\Rightarrow$ some confused with other sources?

Galactic distribution of TeV-detected PWNe

- superimposed on simulated SNR distribution with spiral arms as described by Cordes & Lazio (2002); D uncertainties not shown

young PWNe

offset PWNe

candidate PWNe

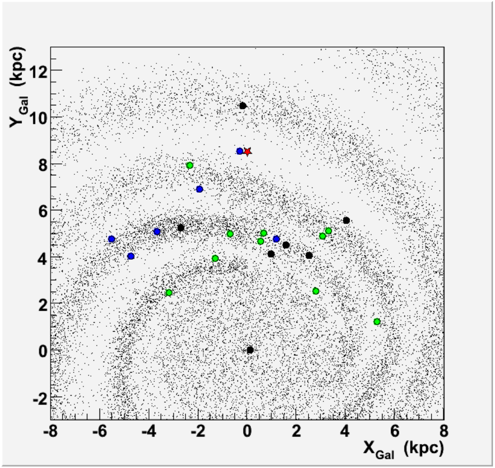

- HESS Galactic plane survey detectability horizon depends on luminosity L_γ and size ℓ; fairly complete to Scutum-Crux arm

Bow-shock pulsar wind nebulae

- PWN expansion in young SNRs is **supersonic** in cold ejecta
- after reverse shock contact, **subsonic** expansion in hot ejecta
- due to birth kick velocity, pulsar motion eventually becomes **supersonic** as SNR cools $\Rightarrow$ PWN bounded by (bow) shock
- in a Sedov SNR, occurs when $R_{\rm PSR} > 0.68\, R_{\rm SNR}$ (van der Swaluw et al. 2003); W44 is likely in this phase

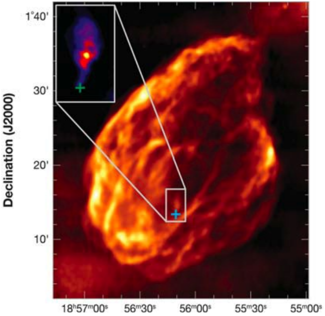

W44 (radio)

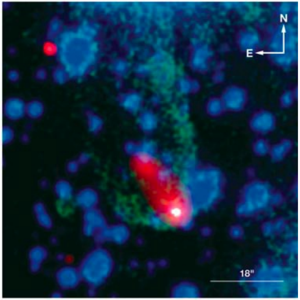

PSR B1957+20 (Hα, X-rays)

Structure of a bow-shock PWN

- at last pulsar crosses SNR shell, forms bow-shock nebula in ISM (with high Mach number)

$$t_{\rm cross} = 44 \left(\frac{E_{\rm SN}}{10^{51}\,{\rm erg}}\right)^{1/3} \left(\frac{n_0}{1\,{\rm cm}^{-3}}\right)^{-1/3} \left(\frac{V_{\rm PSR}}{500\,{\rm km/s}}\right)^{-5/3} \,{\rm kyr}$$

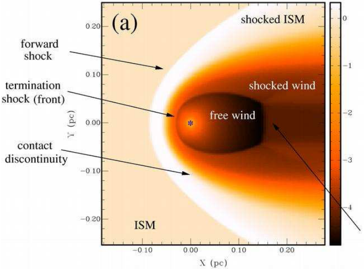

hydrodynamic simulation

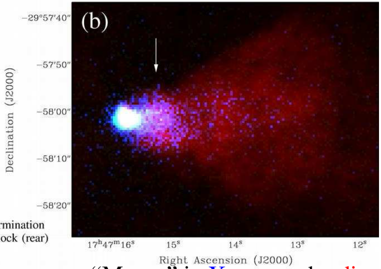

“Mouse” in X-rays and radio

- wind termination shock from balance with (anisotropic) ram pressure ⇒ shock radius varies by factor 1–6 from fore to aft
- shocked neutral ISM emits in Hα; shocked wind in synchrotron

Pulsar wind termination shock geometry

- so far, implicitly considered spherically symmetric pulsar wind
- but pulsar wind nebulae often don't look spherically symmetric!

$\Rightarrow$ 2D (axially symmetric) relativistic MHD simulations

Chandra image of the Crab: bright X-ray torus, jet, inner ring…

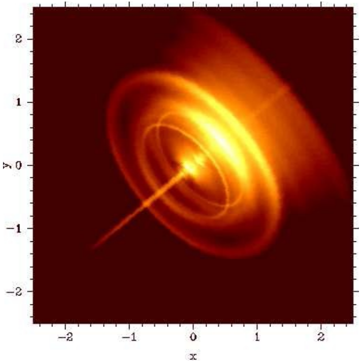

Komissarov & Lyubarsky (2003) RMHD numerical solution, and assumed injected spectrum and synchrotron losses

Anisotropic wind: origin of “jet” and torus

- observed jets a puzzle: collimation inefficient in relativistic wind
- solution (Bogovalov & Khangoulian 2002, Lyubarsky 2002): jet confined in **post-shock** flow, by magnetic hoop stresses and backflow, due to latitude dependence of wind power $f_w \propto \sin^2\theta$
- “jet” then subsonic, as observed : $v \approx 0.3$–$0.7c$

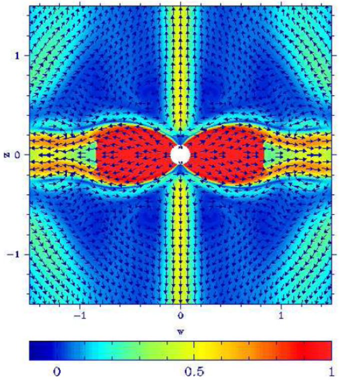

- confirmed by fully RMHD numerical simulations (Komissarov & Lyubarsky 2003, Del Zanna, Amato & Bucciantini 2004, Bogovalov et al. 2005)

⟵ v/c (Komissarov & Lyu. 2003)

- “focusing” of equatorial flow by post-rim-shock “funnel” to supersonic velocities, $v \approx 0.5$–$0.7c$; consistent with optical wisp observations

X-ray torii and jets in PWNe

- many PWNe show X-ray torii (Ng & Romani 2004) and jets

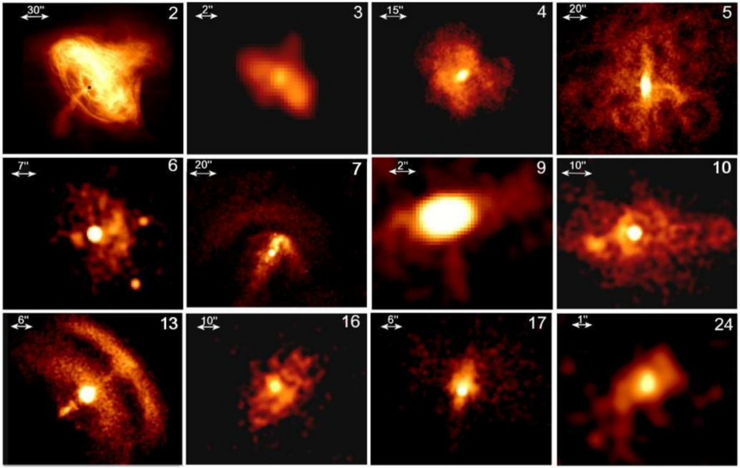

Chandra images of PWNe (Kargaltsev & Pavlov 2008)

- short X-ray synchrotron loss times, harder inner spectral indices: suggest wind (or) termination shock is the acceleration site

Fermi acceleration at the relativistic shock?

- Crab Nebula X-ray spectral index $s_2 \approx 1.1$ suggests injection of power-law spectrum of electrons with $p_2 \approx 2.2$ (before losses)
- X-ray spectra of several other PWNe consistent with this value
- consistent with predictions of **relativistic Fermi acceleration** (Kirk et al. 2000, Achterberg et al. 2001, Keshet & Waxman 2005...)
- this requires small-scale turbulence (voir cours de M. Lemoine)
- apparently realised in particle-in-cell (PIC) simulations of *unmagnetised* shocks

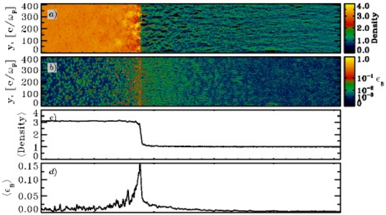

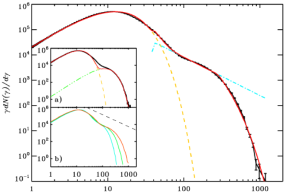

(Spitkovsky 2008)

- but wind magnetisation σ too large? (Sironi & Spitkovsky 2011)
- plerion radio spectra ($s_0 \sim 0$) require a different mechanism

PWN radio spectra and electron pre-acceleration

- Crab radio wisps (Bietenholz et al. 2004) and infrared spectral index map (Gallant & Tuffs 2002) suggest radio-emitting electrons are currently being accelerated near wind termination shock

Resonant ion cyclotron wave acceleration?

- a suggestion (Gallant et al. 2002) is the resonant ion acceleration mechanism of Hoshino et al. (1992), from $\Gamma_{\mathrm{w}} m_e c^2$ to $\Gamma_{\mathrm{w}} m_i c^2$
- implies $\Gamma_{\mathrm{w}} \sim 10^3$ in Crab (vs $\geq 10^6$ in Kennel & Coroniti 1984b)!
- but requires many times Goldreich-Julian current $\dot{N}_{\mathrm{GJ}}$ in ions...

Striped wind reconnection at termination shock?

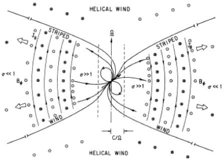

(Coroniti 1990)

- oblique rotator yields alternating B polarities in equatorial wind (striped wind, voir cours de J. Pétri)
- reconnection too slow to annihilate stripes inside Crab termination shock (Lyubarsky & Kirk 2001)?
- Lyubarsky (2003) studied shock in striped wind, suggested that stripes reconnect completely, accelerating electrons with $p_0 \approx 1$
- so far not seen in (1D) PIC simulations (Pétri & Lyubarsky 2007)...

Sources of cosmic-ray positrons and electrons

- *PAMELA* measured positron fraction $e^+/(e^+ + e^-)$ increase inconsistent with secondary origin in cosmic-ray propagation
- combined with cosmic-ray $e^- + e^+$ spectrum measured by *Fermi*-LAT and *HESS*, requires **primary** source of $e^\pm$

- pulsars and wind nebulae are copious sources of relativistic $e^\pm$
- possible cosmic-ray e^+ sources (Chi, Cheng & Young 1996, Zhang & Cheng 2001; Hooper, Blasi & Serpico 2009, ...)
- nearby pulsars can contribute significantly to cosmic-ray electron flux (Büsching et al. 2008, Kawanaka et al. 2009)

N.B. PWNe are not major sources of **hadronic** Galactic cosmic rays

- relativistic nuclei (*Fe*) produced in pulsar magnetospheres
- high $E_{\max}$ possible, but number limited by Goldreich-Julian current $\dot{N}_{\rm GJ}$
- possibly sources of cosmic-rays beyond the "knee" (Giller & Lipski 2002, Bednarek & Bartosik 2004), or of UHECR if born with ms periods (Blasi, Epstein & Olinto 2000; Arons 2003)

Problem : confinement and energy losses

- $e^{\pm}$ accelerated in inner part of PWN (wind termination shock)
- no immediate escape into interstellar medium (ISM) possible (unlike SNR forward shock acceleration); accelerated $e^{\pm}$ then suffer:

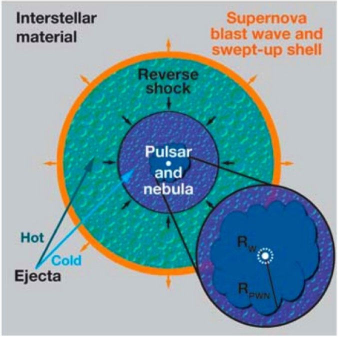

(Gaensler & Slane 2006)

Young composite phase

- confinement by PWN B
- radiative energy losses

Offset PWN phase

- reverse shock "crushing" $\Rightarrow$ enhanced losses
- further expansion $\Rightarrow$ adiabatic energy losses

- only after SNR dissipates into ISM ($\sim 10^5$ yr?) can these particles escape and propagate in the Galaxy
- accurate description much more complicated than simple "escape time" from magnetosphere

Possible solution : bow-shock PWNe?

- due to birth kick velocity, pulsars escape SNR blast wave after time $\sim 4 \times 10^4$ yr; then form **bow shock** PWNe in ISM
- available energy at that time can still be substantial, depending on breaking index n of pulsar (Blasi & Amato 2010)

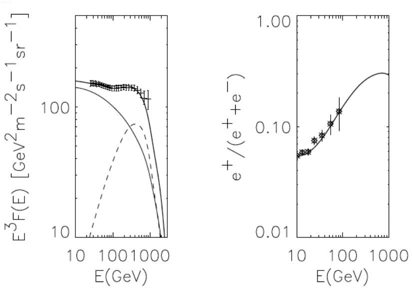

- using empirical PWN $e^{\pm}$ spectrum, Blasi & Amato (2010) can reproduce observed electron spectrum and positron fraction (solid: SNRs; dashed: bow-shock PWNe)
- required efficiency into $e^{\pm}$ $\sim$1% if $n = 3$, but $\sim$30% if $n = 2.5$

Summary and prospects

- pulsar wind nebula spectra compatible with acceleration of a *broken power-law* spectrum of relativistic $e^{\pm}$
- at high E, seems compatible with *relativistic Fermi acceleration*
- low-energy mechanism unclear: stripe reconnection at shock?
- more realistic PIC pulsar wind shock simulations will help

- TeV (and GeV) γ-rays opened new observational window to study PWNe, giving more direct view of accelerated particles
- two broad categories of γ-ray emitting PWNe:
  - young PWNe, typically in composite SNRs
  - offset PWNe, typically with older pulsars
- deeper X-ray and radio observations, new *Fermi* results, and especially future CTA surveys, will yield many more PWNe

- observations of inverse Compton emission reveal dominant Galactic concentrations of high-energy electrons and positrons
- critical issue for a PWN origin of cosmic-ray $e^{\pm}$ is escape from these objects before radiative and adiabatic losses
- more detailed observational and theoretical studies of *late-phase* (e.g. bow-shock) PWNe should help clarify this issue